Konya Mühendislik Bilimleri Dergisi, c. 13, s. 3, 810-821, 2025
Konya Journal of Engineering Sciences, v. 13, n. 3, 810-821, 2025
ISSN: 2667-8055 (Electronic)
DOI: 10.36306/konjes.1617654

A SQUEEZE-EXCITE INTEGRATED NOVEL CNN MODEL FOR BREAST CANCER HISTOPATHOLOGICAL IMAGE CLASSIFICATION

[1,*] Cüneyt ÖZDEMİR, [2] Abdulkerim ÇELİK

[1] Siirt University, Engineering Faculty, Computer Engineering Department, Siirt, TÜRKİYE
[2] On Akçakale Road, 7th km. Opposite to Faculty of Agriculture, Eyyübiye, ŞANLIURFA, TÜRKİYE
[1]cozdemir@siirt.edu.tr, [2]kerimcelik1987@hotmail.com

Highlights

- Novel CNN with squeeze-excite designed for breast cancer classification.
- Benchmarked against 11 transfer learning models on the BreakHis dataset.
- Data augmentation and tuning enhanced model robustness significantly.
- Reliable, high-accuracy tool for early breast cancer detection.

Graphical Abstract

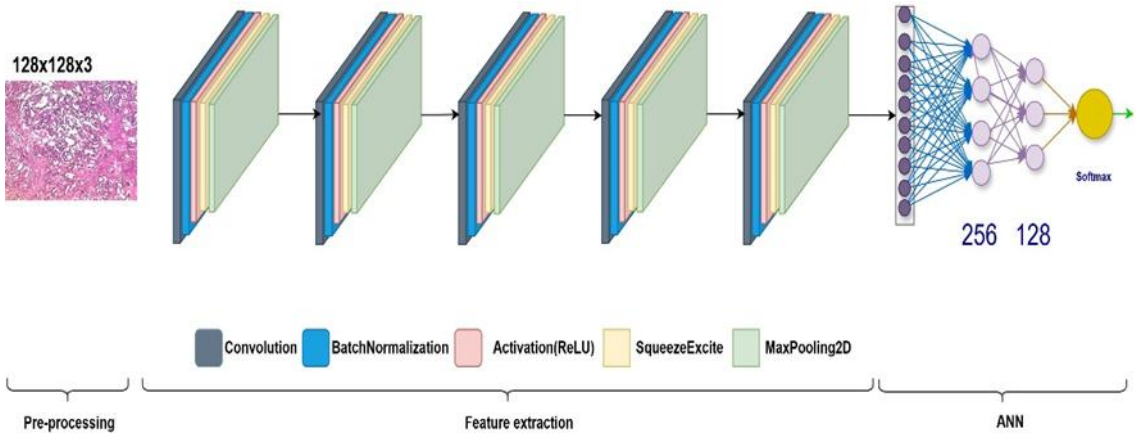

Proposed Novel CNN architecture

*Corresponding Author: Cüneyt ÖZDEMİR, cozdemir@siirt.edu.tr

Konya Mühendislik Bilimleri Dergisi, c. 13, s. 3, 810-821, 2025
Konya Journal of Engineering Sciences, v. 13, n. 3, 810-821, 2025
ISSN: 2667-8055 (Electronic)
DOI: 10.36306/konjes.1617654

A SQUEEZE-EXCITE INTEGRATED NOVEL CNN MODEL FOR BREAST CANCER HISTOPATHOLOGICAL IMAGE CLASSIFICATION

[1,*] Cüneyt ÖZDEMİR, [2] Abdulkerim ÇELİK

[1] Siirt University, Engineering Faculty, Computer Engineering Department, Siirt, TÜRKİYE
[2] On Akçakale Road, 7th km. Opposite to Faculty of Agriculture, Eyyübiye, ŞANLIURFA, TÜRKİYE
[1]cozdemir@siirt.edu.tr, [2] kerimcelik1987@hotmail.com

(Received: 16.01.2025; Accepted in Revised Form: 23.06.2025)

ABSTRACT: Accurate classification of breast cancer histopathological images is essential for early diagnosis and effective treatment planning. This study presents a custom-designed Convolutional Neural Network (CNN) model developed to classify breast cancer histopathological images with enhanced accuracy and reliability. The research began by evaluating the performance of eleven pre-trained transfer learning models, including Xception, InceptionV3, MobileNetV2, and EfficientNetV2B1, using a large histopathological dataset. Hyperparameters such as learning rates, loss functions, optimization algorithms, and data augmentation strategies were meticulously optimized during this process. Among the models, Xception and InceptionV3 exhibited the best performance, achieving accuracy rates of 89.89% and 92.17%, respectively, while MobileNetV2 and EfficientNetV2B1 showed significantly lower results. To address the limitations of transfer learning models and further enhance classification performance, a custom CNN model was developed. The proposed model incorporated advanced architectural features, including squeeze-and-excite mechanisms and group normalization, to improve feature extraction and model stability. This custom CNN achieved superior results, with an accuracy of 93.93%, precision of 94.15%, recall of 93.93%, and an F1-score of 93.98%. The findings emphasize the potential of custom deep learning models in advancing breast cancer diagnostics by providing higher accuracy and generalizability compared to traditional transfer learning approaches. The clinical application of the proposed model could significantly improve early detection and treatment planning by offering healthcare professionals a reliable and efficient diagnostic tool, ultimately contributing to better patient outcomes.

Keywords: *Breast Cancer, Convolutional Neural Networks, Squeeze-Excite, Transfer Learning*

1. INTRODUCTION

Breast cancer continues to be one of the most commonly diagnosed malignancies across the globe and stands as a primary contributor to cancer-related deaths, especially among women [1]. As reported by the World Health Organization (WHO), around 2.3 million new breast cancer cases were diagnosed globally in 2020, resulting in 684,996 deaths, underscoring the significant impact of the disease on global public health. Projections indicate a steady rise in incidence, necessitating advancements in early detection and treatment strategies to improve patient outcomes [2]. Early diagnosis plays a crucial role in enhancing survival rates, emphasizing the need for accurate and efficient diagnostic techniques.

Histopathological examination is the gold standard for diagnosing breast cancer, relying heavily on microscopic analysis of tissue samples. However, this approach is labor-intensive and subject to variability in interpretation, as it depends on the expertise and subjective evaluation of pathologists [3-4]. While traditional imaging techniques such as mammography, ultrasonography, and magnetic resonance imaging (MRI) aid in initial detection [5], [6], histopathological analysis remains indispensable for confirming malignancy. Advances in computational methods, particularly artificial intelligence (AI) and machine learning, have introduced automated approaches to augment diagnostic accuracy and consistency. Deep learning, a subset of machine learning, has emerged as a transformative technology in

***Corresponding Author:** Cüneyt ÖZDEMİR, cozdemir@siirt.edu.tr

medical imaging, demonstrating exceptional performance in tasks such as image recognition and classification [7]. CNNs, in particular, have shown remarkable capabilities in feature extraction and pattern recognition, making them highly suitable for analyzing histopathological images [8], [9]. CNNs leverage hierarchical structures to learn complex features, enabling accurate classification of benign and malignant tissues. Their applications extend to tumor detection, segmentation, and grading, addressing key challenges in cancer diagnostics [10], [11]. The use of transfer learning further enhances the potential of CNNs by leveraging pre-trained models to address specific classification tasks with improved efficiency [12-13]. Several studies have demonstrated the effectiveness of transfer learning models, such as ResNet and VGG, in achieving high classification accuracy [14], [15]. However, existing approaches often face limitations related to dataset variability, model complexity, and generalizability.

This study aims to overcome these limitations by developing and evaluating a custom-designed CNN model optimized with advanced techniques, including squeeze-excite mechanisms and group normalization. The proposed model is designed to outperform existing transfer learning methods by providing higher accuracy, precision, and F1-scores. The methodology focuses on improving classification performance using histopathological images from the BreakHis dataset, enabling more reliable and reproducible diagnostic outcomes.

Some of the main contributions of this study are:

- Development of a custom CNN model optimized with squeeze-excite mechanisms and group normalization techniques to enhance feature extraction and classification performance.
- Evaluation and comparison of eleven pre-trained transfer learning models, including Xception, InceptionV3, MobileNetV2, and EfficientNetV2B1, to benchmark performance.
- Implementation of advanced data augmentation and hyperparameter optimization strategies to improve generalizability and robustness.
- Achievement of higher accuracy, precision, and F1-scores compared to existing transfer learning methods, demonstrating the effectiveness of the proposed approach.

The organization of this paper is as follows: In Section 2, an overview of relevant studies on deep learning techniques for histopathological image classification is presented. Section 3 outlines the materials and methods used, including information about the dataset and the proposed model architecture. Section 4 reviews the experimental results and assesses the model's performance. Finally, Section 5 provides a conclusion, summarizing the key findings, their significance, and offering recommendations for future research avenues.

2. LITERATURE STUDIES

Research on breast cancer classification has seen significant progress with the application of machine learning and deep learning techniques. Various studies have demonstrated the potential of these methods in improving diagnostic accuracy and efficiency.

Veta et al. [16] highlighted the challenges associated with histopathological image analysis and emphasized the need for automated systems to reduce diagnostic variability. Their study formed a foundation for subsequent research focusing on computational methods.

Bacha and Taouali [17] utilized Radial Basis Function Kernel Extreme Learning Machines (RTF-ELM) with Differential Evolution for parameter optimization. Their approach achieved high classification accuracy by combining Kernel Principal Component Analysis (KPCA) for feature selection.

Dai et al. [18] explored ensemble learning methods, specifically Random Forest (RF), to enhance classification performance. Their work demonstrated that ensemble techniques could outperform individual classifiers in terms of robustness and accuracy.

Ara et al. [19] compared various machine learning algorithms, identifying Support Vector Machines

(SVM) and RF as top performers with accuracies exceeding 96%. Similarly, Naji et al. (2021) confirmed the superior performance of SVM classifiers with 97.2% accuracy.

Shukla et al. [20] proposed a segmentation-based approach using Rotation Forest algorithms, achieving high accuracy rates in histopathological image classification. Their work emphasized the importance of image segmentation as a preprocessing step.

Karthiga et al. [21] employed k-means clustering and Discrete Wavelet Transform (DWT) for segmentation, achieving 93.3% accuracy with Support Vector Machine classifiers.

Mukkamala et al. [22] introduced Principal Component Analysis Networks (PCANet) for feature extraction, obtaining 97% accuracy using color-space transformations and SVM classifiers.

George et al. [23] demonstrated the effectiveness of transfer learning using ResNet18, ResNet50, and AlexNet, achieving 96.88% accuracy by combining features through normalization pools.

Han et al. [24] employed BreakHis datasets for multi-class classification, achieving 93.2% accuracy using CNN architectures. Their study highlighted the significance of dataset quality and diversity.

These studies underscore the growing reliance on AI-driven techniques to enhance breast cancer diagnostics. However, challenges related to dataset heterogeneity, feature extraction, and model optimization remain prevalent. This paper builds upon these findings to develop a robust and optimized CNN model addressing these limitations.

3. METHOD

3.1. Datasets

The dataset utilized in this study is the Breast Cancer Histopathological Images (BreakHis) dataset. This publicly available dataset contains 7,909 microscopic images of breast tumor tissues, divided into benign and malignant categories. The dataset was captured using a standard optical microscope with a magnification of 40x, 100x, 200x, and 400x, providing a diverse representation of histopathological variations. Each image in the BreakHis dataset is labeled according to its histological subtype, such as fibroadenoma or ductal carcinoma, allowing for both binary and multiclass classification tasks. The dataset consists of images in PNG format, each with a resolution of 700 x 460 pixels. For the purposes of this study, the data was divided into training, validation, and testing sets using an 80-10-10 split ratio. Stratified sampling was implemented to maintain consistent proportions of benign and malignant samples across all subsets. To improve the model's robustness and ability to generalize, data augmentation techniques such as rotation, flipping, and color variations were applied during training [25]. Figure 1 illustrates an image from the BreakHis dataset used in this study. The image has been magnified for better visualization.

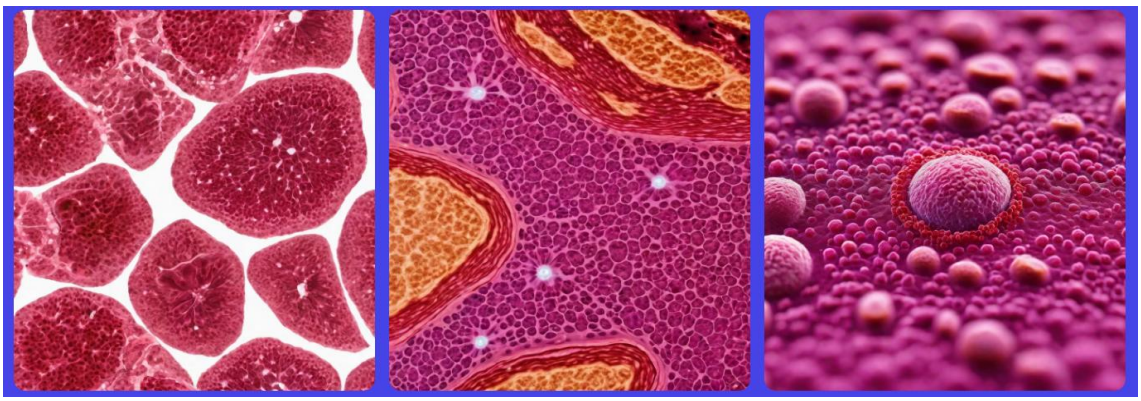

Figure 1. illustrates a representative image from the dataset.

3.2. Performance Metrics

The effectiveness of the proposed approach is measured using various performance metrics, including accuracy, precision, recall (sensitivity), and the F1-score. Recall measures the percentage of actual positive cases correctly detected by the model, reflecting its capacity to identify true positives. Accuracy calculates the proportion of correctly classified instances, both positive and negative, within the entire dataset. Precision evaluates the proportion of true positives among all predicted positive cases, highlighting the reliability of the model's positive classifications. The F1-score, derived as the harmonic mean of recall and precision, offers a comprehensive evaluation by considering both false positives and false negatives. This metric is particularly useful for datasets with class imbalances or uncertain distributions, as it takes all errors into account [26] – [28]. A summary of the mathematical formulas for these metrics can be found in Table 1.

Table 1. Mathematical formulas of the performance parameters.

Parameter	Formula
Accuracy	(TP + TN)/(TP + TN + FP + FN)*100
Recall	TP/(TP + FN)
Precision	TP/(TP + FP)
F-Measure	{2 × (Recall × Precision)}/(Recall + Precision)

In these equations, the terms T, F, P, and N denote True, False, Positive, and Negative, respectively. For example, TP (True Positive) represents the number of correctly classified positive instances, while FN (False Negative) denotes the number of actual positive instances that were misclassified as negative. These metrics provide a comprehensive evaluation framework for assessing model performance.

4. EXPERIMENTAL RESULTS

In the experimental setup, several key hyperparameters were carefully selected to optimize model performance. A batch size of 32 was selected to optimize the balance between memory usage and computational efficiency. The initial learning rate was set to 0.001 and adjusted dynamically using a learning rate scheduler to facilitate better convergence. The Adam optimizer was employed due to its adaptive learning capabilities and reliable performance in deep learning applications. Categorical cross-entropy was used as the loss function, suitable for the multi-class classification problem posed by the dataset. To enhance input data variability and reduce overfitting, data augmentation techniques such as rotation, flipping, and scaling were applied during training. The hyperparameters utilized for model training are detailed in Table 1.

To improve training stability and prevent overfitting, early stopping and learning rate reduction techniques were employed. Specifically, the ReduceLROnPlateau callback was used to adjust the learning rate dynamically based on validation loss (factor=0.2, patience=5, min_lr=0.001), while early stopping was applied with a patience of 5 epochs to halt training when no further improvement was observed. Once the hyperparameters were determined, the images underwent a comprehensive preprocessing phase before being input into the model. Normalization was applied to ensure stable training and improve convergence speed. By scaling the pixel values of the images to the [0,1] range, the training process became more stable, reducing potential gradient explosion issues. Although normalization itself does not directly reduce training time, it contributes to a more efficient learning process, leading to faster convergence and improved model generalization.

Table 2. Hyperparameters used during training of models

Hiperparameters	Value
Learning Rate Reduction	
- Monitor	val_loss
- Factor	0.2
- Patience	5
- Min Learning Rate	0.001
Early Stop	
- Monitor	val_loss
- Patience	5
Model Compile	
- Optimizer	adam
- Loss Function	categorical_crossentropy
- Metrics	accuracy
Train Epoch	200 epoch
Input Image Size	128 x 128
Activation Function	relu

After image preparation, data augmentation was applied to enhance the model's generalization capability and reduce overfitting. This process was implemented using TensorFlow's `ImageDataGenerator` method. The parameters used during the data augmentation process were as follows:

- Rotation Range: 15°
- Horizontal Flip: True
- Shear Range: 0.1
- Fill Mode: 'nearest'
- Zoom Range: 0.1

These augmentation techniques introduced variability in the training data, mimicking potential real-world imaging conditions and improving the robustness of the model.

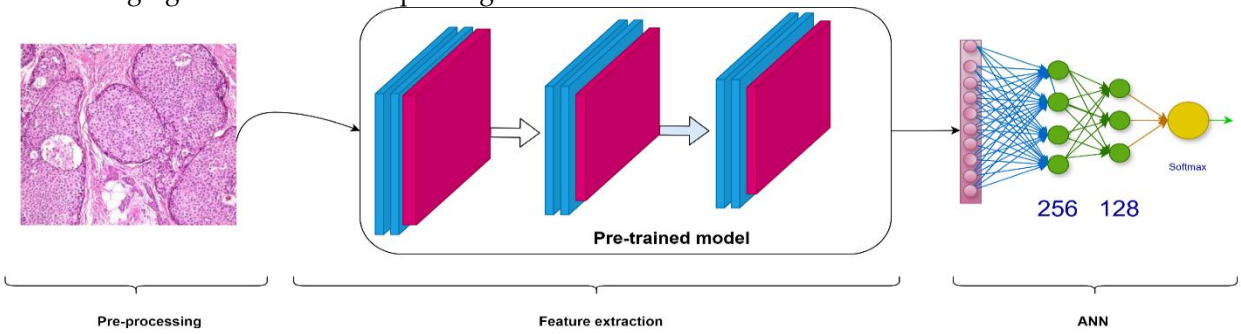

Figure 2. Model architecture

In the initial phase of the experimental studies, transfer learning models were evaluated to analyze their classification performance. Transfer learning leverages pre-trained models, which have been trained on large datasets, to achieve successful results on smaller datasets. In this study, widely used transfer learning models were employed, including Xception, VGG16, ResNet101V2, ResNet152V2, InceptionV3, InceptionResNetV2, MobileNetV2, DenseNet201, NASNetMobile, EfficientNetB1, and EfficientNetV2B1. In this study, the pre-trained transfer learning models were used with their default configurations without any fine-tuning. All layers remained unchanged, and no additional layers were added or frozen during the training process.

The models included in Table 3 were chosen to represent a broad and diverse selection of transfer learning architectures that are frequently used in the literature for medical and histopathological image classification. Our goal was to evaluate both lightweight models (e.g., MobileNetV2, NASNetMobile) and high-capacity models (e.g., InceptionV3, Xception, ResNet152V2) under a consistent evaluation framework. Fine-tuning was not applied to these pre-trained models in order to ensure fairness in the comparative analysis. Fine-tuning typically requires model-specific adjustments—such as deciding how many layers to unfreeze and setting optimal learning rates—which could have led to an unequal or biased performance evaluation. Since our focus at this stage was to assess each model's baseline feature extraction capability, we retained their pre-trained weights and used a unified classification head for all architectures. This approach allowed us to identify their relative strengths without introducing variability arising from model-dependent fine-tuning strategies.

The general architecture of the models used during the experimental studies is illustrated in Figure 2. At the initial stage, feature extraction was performed using the pre-trained transfer learning models. On top of this base architecture, a global average pooling layer was added, followed by two fully connected layers for classification. The first fully connected layer consisted of 256 units, while the second layer contained 128 units, both employing the ReLU activation function. The final classification layer was designed with two output units and used a softmax activation function, tailored to the number of classes being classified. Following the preprocessing and data augmentation steps, experimental results were obtained using the transfer learning models. The outcomes of these experiments, including the performance metrics of the transfer learning models, are presented in Table 3.

The model was trained and evaluated solely on the BreakHis dataset. The dataset was split into 90% training and 10% testing. Additionally, 10% of the training data was set aside for validation.

Table 3. Transfer learning models performance results

Model	Accuracy(%)	Precision(%)	Recall(%)	F1 Score(%)
Xception	89.8905	91.1600	89.8905	90.1038
VGG16	80.4549	80.2839	80.4549	80.3573
ResNet101V2	71.7776	77.8722	71.7776	63.6512
ResNet152V2	75.4844	83.3402	75.4844	76.2543
InceptionV3	92.1651	92.1502	92.1651	92.1570
InceptionResNetV2	84.9200	89.1306	84.9200	85.3941
MobileNetV2	54.5072	66.1422	54.5072	55.3305
DenseNet201	82.8138	83.7568	82.8138	81.4287
NASNetMobile	61.5838	61.8993	61.5838	61.7357
EfficientNetB1	25.5265	29.5405	25.5265	19.7398
EfficientNetV2B1	58.3825	47.0670	58.3825	51.5666

Table 3 presents the performance results of various transfer learning models, evaluated using accuracy, precision, recall, and F1-score metrics. These results provide important insights into the effectiveness of each model in classifying breast cancer histopathological images. Among the models tested, InceptionV3 and Xception exhibited the highest performance. The Xception model achieved an accuracy of 89.89%, precision of 91.16%, recall of 89.89%, and an F1-score of 90.10%. Similarly, the InceptionV3 model slightly outperformed Xception, with an accuracy of 92.17%, precision of 92.15%, recall of 92.17%, and an F1-score of 92.16%. DenseNet201 and InceptionResNetV2 also demonstrated notable performance, achieving accuracy rates of 82.81% and 84.92%, respectively, with high precision and recall values. On the other hand, VGG16 and ResNet152V2 models exhibited moderate results, with VGG16 achieving an accuracy of 80.45% and ResNet152V2 reaching 75.48%. Models such as ResNet101V2 and MobileNetV2 underperformed, with accuracy rates of 71.78% and 54.51%, respectively. NASNetMobile and EfficientNetV2B1 models displayed similarly low performances, achieving accuracy rates of 61.58% and 58.38%, respectively. EfficientNetB1 yielded the lowest performance among all models, with an accuracy of 25.53%, precision of 29.54%, recall of 25.53%, and an F1-score of 19.74%.

Overall, InceptionV3 and Xception outperformed the other models, demonstrating superior generalization and accuracy. Other models showed varying levels of success, highlighting their potential applicability to specific tasks. Following the transfer learning experiments, a custom CNN model was developed to address the unique characteristics of the dataset and further improve classification performance.

The proposed CNN model consists of five convolutional layers, each designed with specific kernel sizes and filter numbers to optimize feature extraction. The first convolutional layer utilizes 64 filters with a 1x1 kernel size, followed by batch normalization and ReLU activation to stabilize learning. Additionally, a squeeze-and-excitation mechanism is applied at this stage to enhance channel-wise feature recalibration, ensuring the network focuses on the most relevant spatial information. This layer concludes with a 2x2 max pooling operation to reduce computational complexity. In the subsequent layers, the number of filters increases progressively to 96, 128, and 256 in the second, third, and fourth convolutional layers, respectively, all using a 3x3 kernel size. Each of these layers follows a structured design pattern, incorporating batch normalization, ReLU activation, squeeze-and-excitation blocks, and max pooling operations to maintain feature consistency and robustness. The final convolutional layer retains 256 filters and adheres to the same configuration, ensuring deep feature extraction. Following the convolutional blocks, the model employs global feature aggregation via a flattening layer, which is then passed through two fully connected layers with 256 and 128 neurons, respectively, both activated using ReLU. A dropout layer with a rate of 0.1 is introduced between the dense layers to mitigate overfitting. The final classification layer consists of two neurons with a softmax activation function, aligning with the binary classification task. The entire architecture was optimized using L2 regularization (λ=1e-4) and the 'he_normal' kernel initializer to enhance weight initialization stability. Hyperparameter tuning was conducted systematically, with a batch size of 32, an initial learning rate of 0.001, and the Adam optimizer. The categorical cross-entropy loss function was used in conjunction with accuracy as the evaluation metric. A full breakdown of the model architecture is provided in Figure 3, illustrating the sequence of convolutional, pooling, and dense layers along with their configurations. This model design effectively balances computational efficiency with high classification accuracy, as demonstrated in the experimental results.

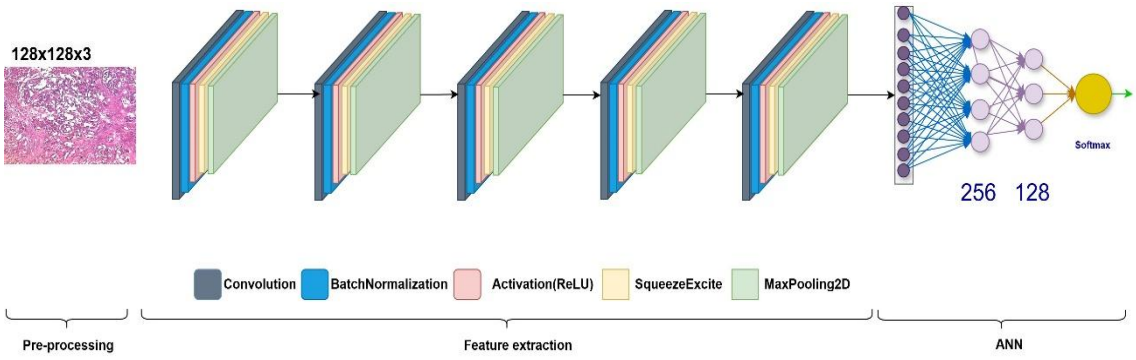

Figure 3. Proposed architecture

To ensure a fair comparison, the proposed model was trained, validated, and tested using the exact same dataset splits and preprocessing pipeline as used in the transfer learning experiments. Specifically, the dataset was split into 80% training, 10% validation, and 10% testing subsets using stratified sampling. Moreover, all hyperparameters (such as learning rate, optimizer, batch size, number of epochs, and data augmentation parameters) were kept consistent with the previous experiments. This allowed for a direct and unbiased comparison between the proposed model and the baseline transfer learning models.

Table 4. Model Performance Results

Model	Accuracy (%)	Precision(%)	Recall(%)	F1 Score(%)
Xception	89.89	91.1600	89.8905	90.1038
InceptionV3	92.16	92.1502	92.1651	92.1570
Proposed Model	93.93	94.1583	93.9343	93.9892

As presented in Table 4, the proposed model outperformed the top-performing transfer learning models, Xception and InceptionV3, from the previous experimental studies. The proposed model achieved the highest metrics across accuracy, precision, recall, and F1-score, demonstrating its superiority over other models. The proposed model attained an accuracy of 93.93%, surpassing all other models and indicating its high capability to make correct predictions. Additionally, its precision of 94.15% highlights its effectiveness in accurately identifying positive classes. The recall rate of 93.93% indicates the model's capacity to accurately identify true positives. With an F1-score of 93.98%, the model shows a well-balanced performance between precision and recall, reinforcing the reliability of the proposed approach. Figure 4 illustrates the accuracy and loss trends of the model throughout both training and validation phases. These graphs offer valuable insights into the model's convergence process and its ability to generalize effectively to new, unseen data.

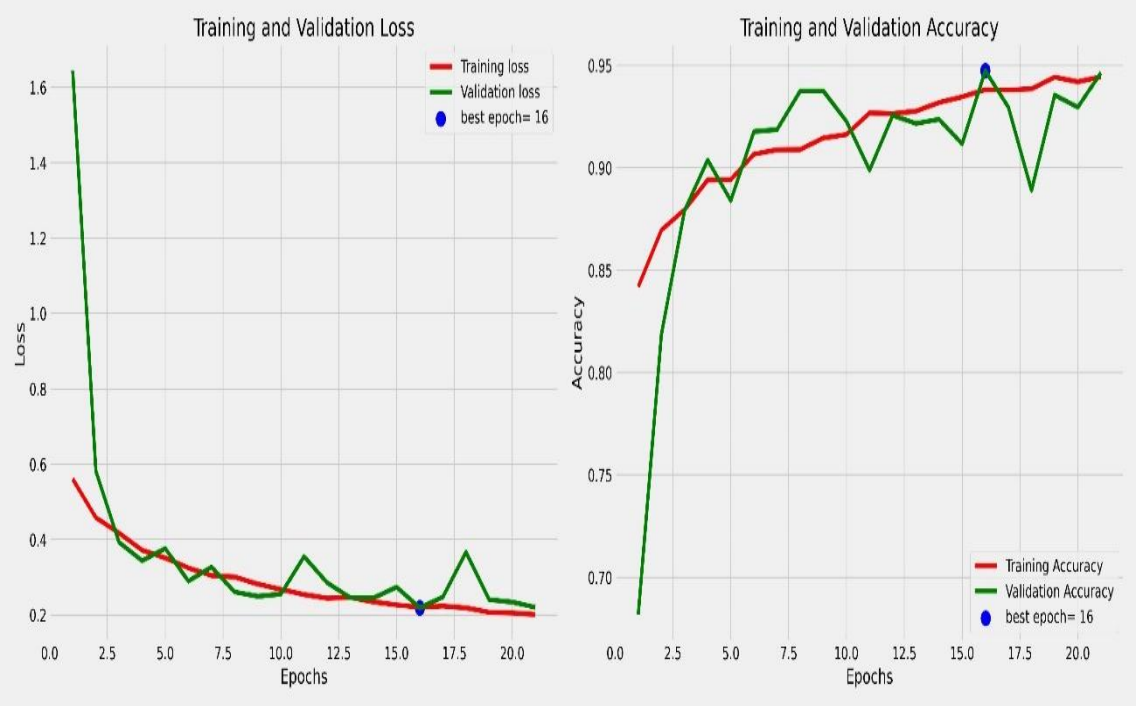

Figure 4. Loss and Accuracy Graph of the Proposed Model

Moreover, the confusion matrix shown in Figure 5 provides a comprehensive examination of the model's classification performance. It illustrates how true positives, true negatives, false positives, and false negatives are distributed, offering a detailed evaluation of the model's classification accuracy.

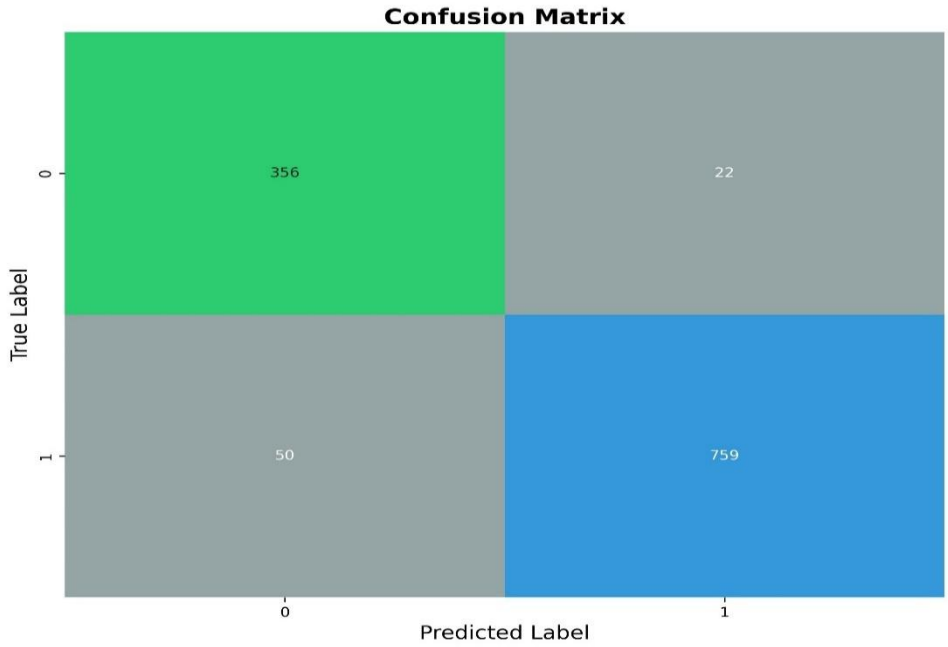

Figure 5. Confusion Matrix of the Proposed Model

The performance of the custom CNN model significantly exceeded that of the transfer learning models. Specifically, the incorporation of squeeze-and-excitation mechanisms and the optimized layer architecture contributed to the improvement in classification accuracy and overall performance. The model not only excelled in terms of accuracy but also achieved higher precision, recall, and F1-scores compared to transfer learning models. This success underscores the ability of the proposed CNN model to generalize more effectively on the dataset and learn complex features more efficiently. These findings reinforce the contribution of this study to the literature, demonstrating the efficiency of the proposed model for specific classification tasks. The superior performance of the custom CNN model establishes it as a reliable and effective solution for histopathological image classification, providing a valuable benchmark for future research.

5. CONCLUSION

In this study, a custom-designed CNN model was developed for the classification of breast cancer histopathological images, and its performance was compared against various transfer learning techniques. The primary objective of this research was to identify the most effective model architecture and hyperparameters for breast cancer detection. The experimental results thoroughly evaluated the performance of widely used transfer learning models, including Xception, VGG16, ResNet101V2, ResNet152V2, InceptionV3, InceptionResNetV2, MobileNetV2, DenseNet201, NASNetMobile, EfficientNetB1, and EfficientNetV2B1.

In the initial phase of the experiments, pre-trained transfer learning models were utilized for image classification tasks. These models, trained on large-scale datasets, were fine-tuned with optimized hyperparameters such as learning rate, loss functions, optimization algorithms, and data augmentation techniques. Data augmentation, aimed at enhancing the model's generalization ability and preventing overfitting, included techniques such as rotation, zooming, cropping, and horizontal flipping. The

models were evaluated using key performance metrics, including accuracy, precision, recall, and F1-score.

Among the transfer learning models, Xception and InceptionV3 demonstrated the highest performance, achieving accuracy rates of 89.89% and 92.17%, respectively, along with superior precision, recall, and F1-scores. Conversely, models such as MobileNetV2 and EfficientNetV2B1 exhibited lower accuracy rates of 54.51% and 58.38%, respectively, indicating limitations in their ability to capture the complexity of histopathological images. To further improve classification performance, a custom CNN model was developed. This model incorporated advanced architectural features, such as squeeze-and-excitation mechanisms and group normalization, to enhance feature extraction and model stability. The architecture consisted of multiple convolutional layers supported by batch normalization and ReLU activation functions. The CNN model presented in this study attained an accuracy of 93.93%, precision of 94.15%, recall of 93.93%, and an F1-score of 93.98%, surpassing all transfer learning models. These outcomes emphasize the efficacy of the proposed architecture and optimization strategies in classifying breast cancer histopathological images. The results of this research carry important implications for advancing automated systems for breast cancer detection. The superior performance of the proposed CNN model underscores the potential of custom deep learning architectures to achieve high accuracy and reliability in medical image analysis. Future research could further enhance these results by exploring more complex model architectures and integrating additional data augmentation techniques. Moreover, the clinical application of such models could provide healthcare professionals with powerful tools for early detection and treatment planning of breast cancer. Incorporating these models into current diagnostic processes could enhance the accuracy and speed of diagnoses, thereby leading to better patient outcomes.

In conclusion, this study demonstrates the potential of deep learning models, particularly custom CNN architectures, to advance breast cancer image classification. The proposed model establishes a robust benchmark for future research and development in this field, highlighting the importance of domain-specific model design and optimization in achieving superior performance in medical imaging tasks.

Declaration of Ethical Standards

The paper is conducted in accordance with ethical standards.

Credit Authorship Contribution Statement

Cüneyt ÖZDEMİR: Conceptualization, Methodology, Software, Validation, Formal analysis, Investigation, Writing – original draft, Writing – review & editing. Conceptualization, Methodology, Software, Validation,

Abdulkerim ÇELİK: Formal analysis, Investigation, Writing – original draft, Writing – review & editing.

Declaration of Competing Interest

The author declares that they have no known competing financial interests or personal relationships that could have appeared to influence the work reported in this paper.

Funding / Acknowledgements

No dedicated funding was received for this research from commercial, public or non-profit entities.

Data Availability

The data set used in this study is given in reference 25.

REFERENCES

[1] H. Sung, J. Ferlay, R. L. Siegel, M. Laversanne, I. Soerjomataram, A. Jemal, and F. Bray, "Global Cancer Statistics 2020: GLOBOCAN Estimates of Incidence and Mortality Worldwide for 36 Cancers in 185 Countries," *CA: A Cancer Journal for Clinicians*, vol. 71, no. 3, pp. 209–249, 2021, doi: 10.3322/caac.21660

[2] M. Arnold, E. Morgan, H. Rumgay, A. Mafra, D. Singh, M. Laversanne, J. Vignat, J.R. Gralow, F. Cardoso, S. Siesling and I. Soerjomataram 2020: "Current and future burden of breast cancer: Global statistics for 2020 and 2040," *The Breast*, vol. 66, pp.15-23

[3] S. Gupta and D. C. Madoff, "Image-guided percutaneous needle biopsy in cancer diagnosis and staging," *Techniques in Vascular and Interventional Radiology*, vol. 10, no. 2, pp. 88–101, 2007

[4] L. He, L. R. Long, S. Antani, and G. R. Thoma, "Histology image analysis for carcinoma detection and grading," *Computer Methods and Programs in Biomedicine*, vol. 107, no. 3, pp. 538–556, 2012

[5] J. M. Seely and T. Alhassan, "Screening for breast cancer in 2018—what should we be doing today?" *Current Oncology*, vol. 25, no. 1, p. 115, 2018, doi: 10.3747/co.25.3770

[6] M. Z. Alom, C. Yakopcic, Mst. S. Nasrin, T. M. Taha, and V. K. Asari, "Breast Cancer Classification from Histopathological Images with Inception Recurrent Residual Convolutional Neural Network," Journal of Digital Imaging, vol. 32, no. 4, pp. 605–617, Feb. 2019, doi: https://doi.org/10.1007/s10278-019-00182-7.

[7] Y. LeCun, Y. Bengio, and G. Hinton, "Deep learning", Nature, vol. 521, no. 7553, pp. 436–444, 2015

[8] M. N. Gurca "Histopathological image analysis: A review," *IEEE Reviews in Biomedical Engineering*, vol. 2, pp. 147–171, 2009 .

[9] S. Otálora, N. Marinr, and M. Atzori, "Combining weakly and strongly supervised learning improves strong supervision in Gleason pattern classification," *BMC Medical Imaging*, vol. 21, no. 1, p. 77, 2021 .

[10] N. Bacanin, T. Bezdan, E. Tubmberger, and M. Tuba, "Optimizing convolutional neural network hyperparameters by enhanced swarm intelligence metaheuristics," *Algorithms*, vol. 13, no. 3, p. 67, 2020

[11] L. Barisoni, K. J. Lafata, S., A. Madabhushi, and U. G. Balis, "Digital pathology and computational image analysis in nephropathology," *Nature Reviews Nephrology*, vol. 16, no. 11, pp. 669–685, 2020 .

[12] A. Alzubaidi, et al., "Breast Cancer Con Using Transfer Learning," *Health Information Science and Systems*, 2020 .

[13] D. Chowdhury, A. Das, A. Dey, S. Sarkar, R. MukkL. Murmu, "ABCanDroid: A cloud integrated android app for noninvasive early breast cancer detection using transfer learning," *Sensors*, vol. 22, no. 3, p. 832, 2022

[14] F. A. Spanhol, L. S. Oliveira, C. Petitjean, and "Breast cancer histopathological image classification using Convolutional Neural Networks," in *2016 International Joint Conference on Neural Networks (IJCNN)*, 2016, pp. 2560–2567, doi: 10.1109/IJCNN.2016.7727519 .

[15] Z. Han, B. Wei, Y. Zheng, Y. Yin, K. Li, and S. Li, "Breaslti-classification from histopathological images with structured deep learning model," *Scientific Reports*, vol. 7, no. 1, p. 4172, 2017 .

[16] M. Veta, J. P. W. Pluim, P. J. Van Diest, and M. A. Viergever, "Breast cancer histopathology image analysis: A review," *IEEE Transactions on Biomedical Engineering*, vol. 61, no. 5, pp. 1400–1411, 2014cha and O. Taouali, "A novel machine learning approach for breast cancer diagnosis," *Measurement*, vol. 187, p. 110233, 2022 .

[17] B. Den, S. Z. Zhu, and W. W. Zhang, "Using random forest algorithm for breast cancer diagnosis," in *2018 International Symposium on Computer, Consumer and Control (IS3C)*, 2018, pp. 449–452 .

[18] S. Ara, A. Das, "Malignant and benign breast cancer classification using machine learning

algorithms," in *2021 International Conference on Artificial Intelligence (ICAI)*, 2021, pp. 97–101 .

[19] M. A. Naji, S. El Filali, . H. Benlahmar, R. A. Abdelouhahid, and O. Debauche, "Machine learning algorithms for breast cancer prediction and diagnosis," *Procedia Computer Science*, vol. 191, pp. 487–492, 2021 .

[20] K. K. Shukla, A. Tiwari, and S. Sharmtion of histopathological images of breast cancerous and non-cancerous cells based on morphological features," *Biomedical and Pharmacology Journal*, vol. 10, no. 1, pp. 353–366, 2017 .

[21] R. Karthiga and K. Narasimhan, "Automated diagnosincer using wavelet based entropy features," in *2018 Second International Conference on Electronics, Communication and Aerospace Technology (ICECA)*, 2018, pp. 274–279 .

[22] R. Mukkamala, P. S. Neeraja, S. Pamidi, T. Babu, and T. Singh, ramework for the binary categorization of breast histopathology images," in *2018 International Conference on Advances in Computing, Communications and Informatics (ICACCI)*, 2018, pp. 105–110 .

[23] K. George, S. Faziludeen, P. Sankaran, and J. K. Paul, "Deep learned nucleusbreast cancer histopathological image analysis based on belief theoretical classifier fusion," in *TENCON 2019-2019 IEEE Region 10 Conference (TENCON)*, 2019, pp. 344–349 .

[24] Z. Han, B. Wei, Y. Zheng, Y. Yin, K. Li, and S. Li, "Breast cancer multi-classification thological images with structured deep learning model," *Scientific Reports*, vol. 7, no. 1, p. 4172, 2017 .

[25] F. A. Spanhol, L. S. Oliveira, C. Petitjean,, L. Heutte, "A dataset for breast cancer histopathological image classification". Ieee transactions on biomedical engineering, 63(7), 1455-1462, 2016.

[26] C. Ozdemir, Y. Dogan, "Advancing early diagnosis of Alzheimer's disease with next-generation deep learning methods". Biomedical Signal Processing and Control, 96, 106614, 2024.

[27] Y. Dogan, "AutoEffFusionNet: A New Approach for Cervical Cancer Diagnosis Using ResNet-based Autoencoder with Attention Mechanism and Genetic Feature Selection". IEEE Access, 2025

[28] Y. Dogan, H. Y. Keles, "Stability and diversity in generative adversarial networks" In 2019 27th signal processing and communications applications conference (SIU) (pp. 1-4). IEEE, 2019.